Available online at www.sciencedirect.com
ScienceDirect
Coastal Engineering 54 (2007) 700–710
Coastal Engineering
An International Journal for Coastal, Harbour and Offshore Engineers
www.elsevier.com/locate/coastaleng

A new formula for the total longshore sediment transport rate

Atilla Bayram [a,*], Magnus Larson [b], Hans Hanson [b]

[a] Halcrow, Inc., 22 Cortlandt St. 33rd Fl., New York 10007, USA
[b] Department of Water Resources Engineering, Lund University, Box 118, S221-00, Lund, Sweden

Received 13 March 2007; accepted 30 April 2007
Available online 7 June 2007

Abstract

A new predictive formula for the total longshore sediment transport (LST) rate was developed from principles of sediment transport physics assuming that breaking waves mobilize the sediment, which is subsequently moved by a mean current. Six high-quality data sets on hydrodynamics and sediment transport collected during both field and laboratory conditions were employed to evaluate the predictive capability of the new formula. The main parameter of the formula (a transport coefficient), which represents the efficiency of the waves in keeping sand grains in suspension, was expressed through a Dean number based on dimensional analysis. The new formula yields predictions that lie within a factor of 0.5 to 2 of the measured values for 62% of the data points, which is higher than other commonly employed formulas for the LST rate such as the CERC equation or the formulas developed by Inman–Bagnold and Kamphuis, respectively. The new formula is well suited for practical applications in coastal areas, as well as for numerical modeling of sediment transport and shoreline change in the nearshore.
© 2007 Elsevier B.V. All rights reserved.

Keywords: Longshore sediment transport; Surf zone; Breaking waves; Field data; Laboratory data; Predictive equation; Engineering application

1. Introduction

The total longshore sediment transport (LST) rate is one of the most commonly required quantities in coastal engineering, needed in problems such as infilling of dredged channels, dispersion of beach fills and placed dredged material, and the morphodynamic response of coastal areas to engineering works. As an example, to maintain navigable waterways along the United States coast, the U.S. Army Corps of Engineers regularly uses analytical and numerical models that employ estimates of the total LST rates in the surf zone. Predicting coastal and barrier island evolution typically requires reliable calculations of the LST. Furthermore, the design of shoreline structures and beach nourishment projects rely on assessment of the impact on the shoreline that is often the result of gradients in the LST rate.

The main objective of the present study is to develop and validate a new predictive formula for the total LST rate to be used in engineering applications. Six high-quality data sets on hydrodynamics and sediment transport collected during both field and laboratory conditions were employed to evaluate the predictive capability of the new formula. The data originated from a series of field campaigns at the U.S. Army Corps of Engineers Field Research Facility at Duck, NC, including the DUCK85 (Kraus et al., 1989), and SandyDuck (Miler, 1998; Miller, 1999) field data collection projects. In addition, the extensive database on the total LST compiled by Schoonees and Theron (1993) was used, together with laboratory data collected at the Large-Scale Sediment Transport Facility (LSTF) of the Coastal and Hydraulics Laboratory of the US Army Engineer Research and Development Center in Vicksburg, Mississippi (Smith et al., 2003). Additionally, two recent field data set obtained by Wang et al. (1998) and Kumar et al. (2004) were used to calibrate and verify the new formula.

In the following, the most commonly applied formulas for calculating the LST rate are first reviewed. The new formula is then derived based on an average concentration and longshore current velocity for the surf zone, where the current may originate from breaking waves, wind, or tides. The six data sets employed to validate the new formula and to determine a predictive relationship for the transport coefficient appearing in

* Corresponding author.
E-mail address: abayram@han-padron.com (A. Bayram).

0378-3839/$ - see front matter © 2007 Elsevier B.V. All rights reserved.
doi:10.1016/j.coastaleng.2007.04.001

the formula are discussed briefly. These data sets comprise 180 field and laboratory cases, and 2/3 of these cases were used to calibrate the coefficient in the new formula and 1/3 of the cases were used to examine the predictive capability of the formula. It is demonstrated that the transport coefficient is a function of the Dean number. Finally, the new formula is compared with the verification database (i.e. 1/3 of the cases) together with three other formulas, namely the formula proposed by Inman and Bagnold (1963), the CERC equation (USACE, 1984), and the formula by Kamphuis (2002).

2. Previous equations for the total longshore transport rate

The most widely used formula in coastal engineering practice for the total LST rate is the CERC equation (USACE, 1984). It is based on the principle that the volume of sand in transport, Q_{lst} is proportional to the longshore wave power per unit length of the beach and given by,

$$Q_{\mathrm{lst}} = \frac{\rho K \sqrt{g/\gamma_b}}{16(\rho_{\mathrm{s}} - \rho)(1-a)} H_{s,b}^{2.5} \sin(2\theta_b) \tag{1}$$

where Q_{lst} is the longshore transport rate in volume per unit time, K is an empirical coefficient, ρ is the density of water, ρ_{s} is the density of sand, g is acceleration due to gravity, a is the porosity index ($\cong$0.4), $H_{s,b}$ is the significant wave height at breaking, γ_{b} is the breaker index ($=H_{\mathrm{b}}/h_{\mathrm{b}}$), and θ_{b} is the wave angle at breaking. The shore protection manual (USACE, 1984) recommends a value of K=0.39 that was derived from the original field study by Komar and Inman (1970) using tracers. In recent studies, Schoonees and Theron (1993, 1996) re-examined the 46 most reliable of the 240 existing field measurements that have been compiled to determine a K-value of approximately 0.2.

Inman and Bagnold (1963) proposed a theory in which wave energy was expended to suspend and support the sand above the bottom, and any unidirectional current superimposed on the orbital wave motion could transport sand and produce a net drift in the direction of the current. The transport formula derived based on their theory may be expressed as,

$$Q_{\mathrm{lst}} = \frac{K_{\mathrm{b}}}{(\rho_{\mathrm{s}} - \rho) g (1-a)} C_{\mathrm{gb}} E_{\mathrm{b}} \cos\theta_{\mathrm{b}} \left(\frac{V_{\mathrm{l}}}{u_{\mathrm{o}}}\right) \tag{2}$$

where E_{b} is the breaking wave energy, C_{gb} is the wave group velocity at breaking, V_{l} is the longshore current velocity (in practice measured at the mid-surf-zone location), and u_{o} is the maximum horizontal bottom orbital velocity of the waves at the breaker zone. The coefficient K_{b} is a dimensionless constant, which is given as 0.25 based on field data collected at different beach locations in United States and Japan (Komar, 1998).

Kamphuis (1991) developed a relationship for estimating LST rates based primarily on physical model experiments. The formula which Kamphuis (2002) found to be applicable to both field and laboratory data is,

$$Q_{\mathrm{lst},m} = 2.27 H_{s,b}^{2} T_{\mathrm{p}}^{1.5} m_{\mathrm{b}}^{0.75} D_{50}^{-0.25} \sin^{0.6}(2\theta_{\mathrm{b}}) \tag{3}$$

in which $Q_{\mathrm{lst},m}$ is the transport rate of immersed mass per unit time, T_{p} is peak wave period, m_{b} is the beach slope near the breaking, i.e., the slope over one or two wavelengths seaward of the breaker line, and D_{50} is the median grain size. The immersed weight is related to the volumetric rate as $Q_{\mathrm{lst},m}=(\rho_{\mathrm{s}}-\rho)(1-a)Q_{\mathrm{lst}}$. The Kamphuis formula is appealing since it includes the wave period and beach slope, which both influences wave breaking, and the grain size, which should be an important factor for the mobilization and transport of sediment.

3. Development of a new formula for LST rate

3.1. Sediment transport formula

Most of the existing formulas on the LST only consider wave-generated currents (e.g., CERC (USACE, 1984), Kamphuis (1991) formula), and disregard other mechanisms, such as wind and tidal currents, that could influence the LST. Examples of the importance of wind, which is not considered in most of the longshore transport formulas, are furnished by the studies of Ciavola et al. (1997) and Masselink and Pattiarachi (1998). In the first paper, a six-fold increase in LST rate on a Portuguese beach occurred when locally brisk winds blew in the same direction as the longshore currents. In the latter paper, sea breeze on Western Australian beaches was observed to increase the longshore suspended sediment transport by a factor of one hundred. Thus, there is a need to have a formula that includes other than wave-generated currents. At the same time, major physical factors such as sediment and wave characteristics should be included in the formula. For example, the Inman–Bagnold formula that allows the inclusion of wind- or tide-driven currents, does not exhibit any grain-size dependence. Finally, in order to provide reliable and robust predictions of the LST rate a formula should be validated with an extensive data set that covers a wide range of wave, sediment, and beach conditions.

Because of the limitations in existing formulas, an effort was made in the present study to derive an alternative formula for the LST rate. This formula should (1) apply not only to wave-generated currents, but also to the case of sediment transport by wind and tidal currents; (2) include major physical factors governing LST; and (3) be validated with an extensive data set covering a wide range of conditions.

Suspended sediment is assumed to be the dominant mode of transport in the surf zone, since the bottom sediment is stirred up (suspended) by strong wave action. Generally, in the nearshore zone, it is believed that breaking waves suspend most of the transported sediment, whereas much less sediment is transported outside the surf zone. Thus, in the new formula, the presence of breaking waves is required to mobilize sediment, whereas any type of current (e.g., from breaking waves, wind, and tide) can transport the sediment. The wave breaking stirs up sediment and maintains an average concentration distribution $c(x,z)$ in the surf zone (c in units of m^3 sediment/m^3 water). The total amount of work (W) needed to keep the sediment in suspension is given by the

product of the concentration and the submerged weight of the particle with the fall speed w_s,

$$W = \int_0^{x_b} \int_{-h(x)}^{0} c(x,z)(\rho_s - \rho) g w_s \mathrm{d}z\mathrm{d}x \tag{4}$$

where x is a cross-shore coordinate originating at the shoreline and taken positive offshore (b denotes the break point), z a vertical coordinate originating at the still-water level, and h water depth. The flux of wave energy towards shore is F (=EC_g) and a certain portion ε of this energy is used for the work W, that is, $W=\varepsilon F$, which yields (compare with Larson and Hanson, 1996; Katayama and Goda, 2000; Larson and Bayram, 2005):

$$\varepsilon F = (\rho_s - \rho) g w_s \int_0^{x_b} \int_{-h(x)}^{0} c(x,z)\mathrm{d}z\mathrm{d}x. \tag{5}$$

If the LST rate is taken to be the product of concentration and longshore current velocity (V), the total transport rate is given by:

$$Q_{lst} = \int_0^{x_b} \int_{-h(x)}^{0} c(x,z) V(x,z)\mathrm{d}z\mathrm{d}x. \tag{6}$$

Assuming a constant (or representative) longshore current velocity and replacing the integral with the fraction of the incoming wave energy that is used for keeping the sediment in suspension yields,

$$Q_{lst} = \frac{\varepsilon}{(\rho_s - \rho)(1-a) g w_s} F \bar{V} \tag{7}$$

where $\bar{V}$ is the mean longshore current velocity over the surf zone and the porosity (a) was added in the denominator. The value of the transport coefficient (ε), which expresses the efficiency of the waves in keeping sand grains in suspension, may be determined using high-quality field and laboratory data or through some theoretical considerations. In a perfect model of the LST ε would be a universal constant, but because of the simplifications in the physical model employed to describe the processes involved it is expected that ε might vary depending on wave and sediment conditions. The new formula may include any type of current and the effect of sediment size is described through the fall speed in the denominator.

3.2. Longshore current and wave-energy flux

In order to compute the LST, the mean longshore current and the wave-energy flux must be known (see Eq. (7)). Wave information is typically available (measured or hindcasted) to estimate the wave-energy flux, and if the current has been measured, it is straightforward to calculate Q_{lst}. However, in general, current measurements will not be available, but $\bar{V}$ has to be obtained from calculations. In the present study, measurements of the current were available for some of the data sets, whereas for the other data sets $\bar{V}$ were calculated from the wave and beach profile characteristics. In the following, a brief review is given of the simple longshore current model used to estimate $\bar{V}$. When fitting Eq. (7) to data and estimating optimum values on ε, these values will depend to some extent on the equation employed for computing $\bar{V}$. Thus, preferably the same longshore current model as discussed below should be used to compute $\bar{V}$, if the empirical formula recommended for ε is utilized (Eq. (23)).

By applying a simple alongshore momentum equation, linearized friction, and neglecting lateral mixing, an expression for the longshore current can be written as (Larson and Kraus, 1991),

$$\frac{2}{\pi} \rho c_f u_o V = \frac{\mathrm{d}S_{xy}}{\mathrm{d}x} \tag{8}$$

where c_f is the friction coefficient, u_0 is the bottom orbital velocity, and S_{xy} is the radiation stress directed alongshore and transported onshore. Assuming shallow-water conditions, the following relationships hold:

(a) Linear wave theory gives a representative value of the maximum near-bottom wave orbital velocity,

$$u_o = \frac{H}{2}\sqrt{\frac{g}{h}} \tag{9}$$

where H is the wave height and h is the water depth.

(b) Within the surf zone, the ratio of wave height to water depth is taken as,

$$H = \gamma_b h \tag{10}$$

in which the breaker index γ_b is taken to be 0.78.

(c) The longshore component of radiation stress (Longuet-Higgins, 1970) is given by:

$$S_{xy} = \frac{1}{16} \rho g H^2 \sin 2\theta \tag{11}$$

(d) The Snell's law for refraction

$$\frac{\sin\theta_b}{\sqrt{gh_b}} = \frac{\sin\theta}{\sqrt{gh}.} \tag{12}$$

Substituting the above expressions (Eqs. (9)–(12)) into the governing equation (Eq. (8)), and employing a Dean's equilibrium beach profile ($h=Ax^{2/3}$, where A is a shape parameter, (Van Rijn, 1993)), the longshore current velocity is given by:

$$V = \frac{5}{24} \frac{\pi \gamma_b \sqrt{g}}{c_f} A^2 \frac{x^{1/3}}{\sqrt{h_b}} \sin\theta_b. \tag{13}$$

In Eq. (13), V varies across the profile, and the average current is determined from:

$$\bar{V} = \frac{1}{x_b} \int_0^{x_b} V \mathrm{d}x = \frac{5}{32} \frac{\pi \gamma_b \sqrt{g}}{c_f} A^{3/2} \sin\theta_b. \tag{14}$$

One contribution missing in the preceding equation is the influence of the lateral mixing, which would tend to smooth out

the velocity profile given by Eq. (13), particularly in the vicinity of the breaker line. The effect of the lateral mixing on the mean current will be less pronounced, and for the present purpose, the accuracy should be sufficient. Uncertainty also enters through the friction coefficient (c_f) that in the general case is dependent on the flow and sediment properties but is taken to be a constant here (0.005 based on Larson and Kraus, 1991). Another simplification in deriving Eq. (14) is the use of a single representative wave. In reality, waves are multi-directional and random which will affect the magnitude of the longshore current as well as the width of the surf zone. The uncertainty in the estimate of $\bar{V}$ will be reflected in the scatter produced by Eq. (7) when compared to the data.

For a wave that is not normally incident to the shoreline, the wave-energy flux is given by,

$$F_b = E_b C_{gb} \cos\theta_b \tag{15}$$

where E_b is the wave energy per unit crest width, C_{gb} is the group velocity, and index b denotes incipient breaking. Using linear wave theory, the following relationships hold:

$$E_b = \frac{1}{8}\rho g H_b^2 \tag{16}$$

$$C_{gb} = \sqrt{g\frac{H_b}{\gamma_b}}. \tag{17}$$

Neglecting energy dissipation seaward of the surf zone (i.e., bottom friction), the wave-energy flux needed in Eq. (7) can be estimated at any depth since $F=F_b$.

3.3. Comparison between new formula and CERC equation

It is interesting to compare the new formula with the CERC equation for the case of wave-generated current only in order to derive a theoretical expression for ε in terms of the coefficient K. Kriebel et al. (1991) showed that the relationship between A and w_s may be described by:

$$A = \frac{9}{4}\left(\frac{w_s^2}{g}\right)^{1/3}. \tag{18}$$

Employing Eqs. (14), (15), and (18) in Eq. (7) and equating it to Eq. (1) yields:

$$\varepsilon = \frac{256}{135}\frac{c_f}{\gamma_b \pi}K. \tag{19}$$

Using the employed values from the longshore current modeling yields $\varepsilon = 3.9\times10^{-3}\ K$, which gives a representative value of $\varepsilon = 1.5\times10^{-3}$ for $K=0.39$. Note that under the above assumptions concerning the wave-generated longshore current and the profile shape, the new formula reduces exactly to the CERC equation, if Eq. (19) holds.

4. Longshore sediment transport data

Six high-quality data set on the LST rate were employed to determine the optimum value of the transport coefficient (ε) and to test the predictive capability of the new formula. In total, the six data sets consist of 180 cases. Of these cases, 2/3 was used to determine the transport coefficient and the rest of the data (i.e., 1/3 of the cases) were used to evaluate its predictive capability. The first group of data set is denoted as the "calibration data set" and the latter as the "verification data set", hereafter. Division of the data into the calibration and verification sets was done by random selection from each of the original six data sets.

When identifying data sets suitable for calibrating and verifying the new LST formula, accuracy and reliability in the measurements were primary criteria for inclusion. The data sets consist of wave properties, sediment characteristics, and the longshore transport rate at a variety of locations. Basically, all of the data sets involved LST induced by wave breaking, and no data were collected where tide- or wind-driven currents were significant. Brief background descriptions concerning the experiments are provided in the following sections. For further details regarding the experiments, the reader is directed to the original papers.

4.1. Large-Scale Sediment Transport Facility (LSTF) data

The experiments were conducted in the LSTF at the Coastal and Hydraulics Laboratory of the U.S. Army Engineer Research and Development Center in Vicksburg, Mississippi (Smith et al., 2003; Wang et al., 2002). Irregular waves ranging from 0.16 m to 0.25 m in energy-based significant wave height and 1.5 to 3.0 s in peak spectral wave period were generated at a 10° angle to shore-normal. Two types of breakers, namely plunging and spilling, were observed during the experiments. The beach consisted of very well-sorted fine quartz sand with a median grain size (D_{50}) of 0.15 mm. The longshore current generated by the obliquely incident waves was circulated with 20 turbine pumps through the 20 flow channels at the updrift and downdrift end of the basin. Wang et al. (2002) provided detailed discussions of the experiments in their paper.

Ten Acoustic Doppler Velocimeters (ADVs) were used to measure the total velocities (wave orbital velocities and unidirectional longshore currents). Sediment fluxes were obtained from twenty 0.75 m wide traps situated at the downdrift end, which covered the entire surf zone. Eighteen traps were installed in the downdrift flow channels and two additional traps were located landward of the first flow channel to predict LST rate across the surf zone including the swash zone. Each trap was equipped with three load cells, which were capable of weighing the amount of trapped sand. The total longshore transport rate was computed by summing the sediment flux measured in all of the traps. The test conditions

and measured quantities obtained from the LSTF study are given in Table 1.

4.2. Duck85 field data

The experiments were conducted at the Field Research Facility (FRF) of the U.S. Army Corps of Engineers (USACE), located on the Atlantic Ocean near the village of Duck, North Carolina, USA (Kraus et al., 1989). During the Duck85 field data collection project, the longshore transport was measured using portable streamer traps in the surf zone (depth about 1 m). The experiments were performed under swell conditions with moderate breaking wave heights ($H_{s,b}$) in the range of 0.8 m to 1.2 m and T_p in the range of 9 to 13.1 s. Waves were predominantly from the southern sector producing a longshore current velocities between 0.1 m/s to 0.3 m/s to the north, based on measurement results of electro-magnetic current meters at two locations (i.e., each sensor at 0.2 m to 0.3 m above bed). The wave height distribution throughout the surf zone was measured by filming the water surface elevations at various poles jetted into the seabed on a line crossing the surf zone.

The nearshore bathymetry remained predominantly two-dimensional during the experiments and the foreshore had a steep beach face covered by pebbles, where no sediment was observed to move. Seaward of the beach face, the inner surf-zone profile had a gentle slope with a typical depth of 1 m increasing to 2 m at the seaward edge of surf zone. The portable streamer traps, that were used to measure the LST rate, consisted of flexible polyester filter cloth (0.105 mm mesh) which allows water to pass through but retains sediment of the nominal diameter larger than the mesh size. Each streamer cloth was 2 m long and its mouth was 0.15 m wide and 0.09 m high. The traps consisted of a vertical array of five streamer clothes, and the first streamer was placed on the bed and collected sediment moving into it as bed load together with suspended load. Six or seven traps were simultaneously deployed on a line crossing the surf zone with the streamer mouths facing into the longshore current (sampling time of about 5 to 10 min). The width of the surf zone was about 25 to 39 m, and the suspended sand size caught in the streamers was between 0.15 and 0.2 mm.

Table 1
Longshore sediment transport database

Data source	$H_{s,b}$ (m)	T_p (s)	D_{50} (mm)	θ_b (degree)	$Q_{measured}$ (m^3/s)
LSTF data (Smith et al., 2003)	0.2–0.3	1.5–3.0	0.15	6.0–7.0	4×10^{-5}–1.1×10^{-4}
Duck85 data (Kraus et al., 1989)	0.8–1.2	9.0–13.1	0.17	–[a]	2.8×10^{-4}–1.9×10^{-3}
SandyDuck data (Miller, 1999)	1.7–4.3	6.0–13.0	0.17	5.0–23.0	9.6×10^{-2}–0.6
Wang et al. (1998) data	0.2–1.1	3.0–10.5	0.2–2.25	2.0–20.0	6.4×10^{-5}–4.7×10^{-3}
Kumar et al. (2004) data	0.5–1.2	5.0–18.0	0.18–0.2	5.0–18.0	1.2×10^{-3}–2.0×10^{-2}
Schoonees and Theron (1993) data	0.2–3.4	5.0–12.0	0.18–1.0	2.0–35.0	8.6×10^{-4}–0.14

[a] Wave angle at breaking was not measured during the Duck85 experiment.

The eight longshore transport rates recorded were in the range of 1.5 kg/s to 6.5 kg/s. Hydrodynamic conditions and transport rates observed during the Duck85 field experiment are summarized in Table 1.

4.3. SandyDuck field data

During the SandyDuck field data collection project, also performed at the FRF, direct measurements of velocities and suspended sediment concentrations were conducted at a minimum of nine positions across a barred profile in wave heights up to 3.5 m (energy-based significant wave height; H_{m0}) to provide an estimate of the total longshore suspended sediment transport (Miller, 1999). The wave climate in the fall at the FRF is dominated by the violent "northeaster" and the close passage of tropical hurricanes. Tides are semi-diurnal, with a spring tide range of 1.2 m. The bed profile is composed of fine to coarse sand, and the beach face consists of bimodal sand with a main component around 0.25 mm. Sediment in the bar/through region is more unimodal with a mean of 0.17 mm, and seaward of the storm bar the sediment is well-sorted with a mean of 0.12 mm. The overall bed slope in the surf zone between the shoreline and the 5 m depth contour is about 1 to 40 ($\tan\beta=0.025$) and 1 to 65 ($\tan\beta=0.015$) between the shoreline and the 8 m depth contour. Wave measurements are available from a directional pressure gage array located in a depth of 8 m offshore and north of the research pier. The velocity and concentration measurements were taken by means of instruments attached to the lower boom of a track-mounted crane (Sensor Insertion System; SIS) stationed on the pier. The SIS can place instrumentation on the bottom in depths up to 9 m and 15 m away from the pier pilings.

Accurate determination of the LST requires sampling at many cross-shore positions under stationary hydrodynamic conditions. To minimize water level fluctuations due to the tide, measurements were made within 1.5 h of high or low tide. Using data records of 8 min, about 10 cross-shore positions could be sampled. The vertical array of instruments consisted of eight optical (OBS) concentration sensors and four electro-magnetic current meters. The lowest (bottom) concentration sensor was nominally 3 cm above the bed, but the distance varied from 2 to 5 cm. The upper concentration sensor was about 50 cm below the wave trough level. The OBS sensors were post-experiment calibrated against a composite of suspended sediment samples collected during the storms using 0.1 mm mesh streamer traps mounted on the SIS. Prior to computing sediment flux, the "turbidity" offset was removed from the OBS signal.

The longshore suspended sand transport at each position was computed by multiplying the instantaneous concentration with the instantaneous longshore current velocity and time averaging the products. Most local flux values have the same direction as the local mean longshore current, but some flux values are in the opposite direction (e.g., on the 27th of March 1996 and the 2nd of April 1996). The flux from the bottom sensor to the bed was assumed constant. The local longshore fluxes were integrated along the cross-shore bed profile, and the flux between the

innermost measurement location and the mean shoreline position was assumed constant. The bed-load transport was not measured. Most of the longshore transport occurred in the outer surf zone seaward of the 3 m depth contour during the storm. The transport in the swash zone was not included, but during storms, it was likely that the sampled zones included most of the transport. Hydrodynamic conditions observed during the SandyDuck field experiment are listed in Table 1.

4.4. Schoonees and Theron data compilation

Schoonees and Theron (1993) made an inventory of the available data sets on LST rates, resulting in 123 data sets that included transport rates and wave and sediment characteristics. The data were collected on beaches from a variety of sites all around the world, encompassing particulate (non-cohesive) sediment (including sand, gravel, and shingle) transported alongshore from the swash zone across the surf zone to deep water. Transport data were derived using three different methods, namely tracers, samplers and traps, and measured morphological volume change. The time period of data collection varied markedly between data sets, where longer time periods imply a greater variability in the forcing conditions. Short-term data sets implied that the wave conditions were relatively constant during the measurements, at least in a statistical sense.

For the majority of the short-term data sets the wave heights were smaller than 1.8 m and the waves were breaking at an angle less than 20° to shore-normal. The longshore transport rates were below 50 kg/s. Schoonees and Theron (1993) concluded that most data sets based on short-term measurements fall in the range of mild wave conditions for fine to coarse sand. In the present study, the focus was on data sets based on short-term measurements using direct sampling methods. The data sets collected using tracers were not considered reliable enough because of the difficulties in deriving transport rates from the horizontal and vertical transportation of the tracer material (suspended transport is typically underestimated). In addition, morphological volume change methods were disregarded as the resulting transport rates often are due to strongly varying wave conditions because the data was collected over a significant time period. Table 1 summaries the hydrodynamic and sediment conditions in the database compiled by Schoonees and Theron (1993).

4.5. Wang et al. surf-zone sediment transport experiments

Wang et al. (1998) performed field experiments along the Southeast coast of the United States and the Gulf Coast of Florida between September 1993 and May 1995. They measured the total rate of LST in the surf zone, mostly by using streamer traps. Twenty-nine streamer trap experiments and one short-impoundment experiment were performed under low-energy conditions. The selected sites represented a wide range of morphodynamic and hydrodynamic conditions. Seven out of the 29 trap experiments were performed on barred coasts with waves breaking on the longshore bar. Eighteen trap experiments were carried out on coasts with negligible offshore bar influence on the wave breaking. The remaining experiments were done in the inner surf zone on barred coasts, because of operational difficulties due to high waves and large offshore depths. Twelve field sites among the 29 field sites had a plunge step at the breaker line or at the secondary breaker line for the case of the barred coasts.

Based on measured wave heights from video images, the root-mean-square wave height (H_{rms}) was calculated and it ranged from 0.1 to 0.8 m during the experiments (low wave-energy conditions). The measurements of the incident wave angle were in the range of 2° to 35°. The peak spectral wave period varied from less than 3 s to more than 10 s. The surf-zone width ranged from as narrow as 2 m to as wide as 54 m, and the average surf-zone width was 14 m with a standard deviation of 13 m, indicating great variability. Sediment properties varied from one site to another, with the average bottom sediment grain size ranging from 0.17 mm to 2.25 mm. The overall bed slope in the surf zone were between 1 on 75 (tan β=0.013) and 1 on 5 (tan β=0.214). The trap measurements were made under plunging, spilling, and collapsing wave conditions. Streamer traps used in their study were similar to the ones used in the Duck85 study (Kraus et al., 1989). The streamer cloth was 2 m long and its mouth was 0.15 m wide and 0.09 m high. The mesh size of the sieve cloth was 63 μm. Hydrodynamic and morphodynamic conditions observed during the field experiments are listed in Table 1.

4.6. Kumar et al. surf-zone sediment transport experiment

Kumar et al. (2004) performed field experiments along the southwest coast of India between February and May 1990. During the field campaign, both the cross-shore and vertical distribution of the sediment transport rate were measured with traps deployed on a 4-km long beach. Breaking wave parameters were estimated from data collected using a directional wave buoy in 16 m water depth. Wave height at breaking varied from 0.5 to 1.2 m with an average of 0.8 m, and wave heights were greatest ($H_{s,b}$ >1 m) during May, just before the start of the southwest monsoon. The peak spectral wave period varied from 5 s to 18 s, and the average breaking wave angle was 5.6°. Average surf-zone width was about 40 m during the measurements. The tides are predominantly semi-diurnal with an average spring tide of 2 m and neap tide of 0.25 m during the measurement period. The longshore current velocities were measured at the trap locations. The velocity varied from 0.1 m/s to 0.6 m/s with an average value of 0.3 m/s.

Two different traps were used to measure the LST rates. Mesh traps having circular openings were used for measuring the suspended load transport and streamer traps were used for measuring the bed-load transport. The streamer traps used in this study were similar to the ones used in Duck85. The opening of the trap was 0.2 m wide, 0.15 m high, and rectangular in shape. The filter cloth mesh opening size was 90 μm and the opening of the mesh trap was 0.034 m. Total measured LST rates across the surf zone varied from 1.86 kg/s to 39 kg/s.

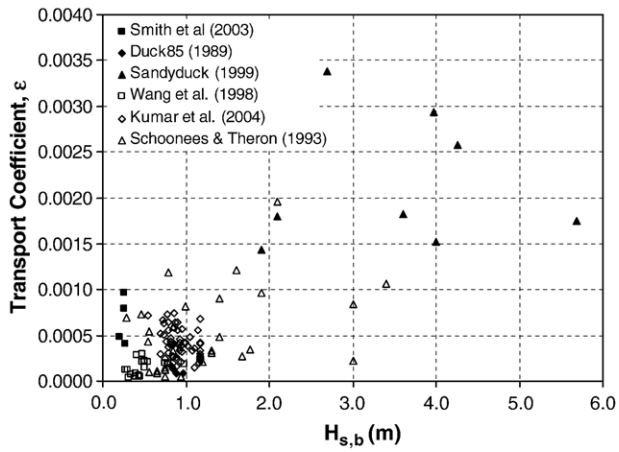

Fig. 1. Relationship between transport coefficient, ε and significant wave height at breaking, $H_{s,b}$.

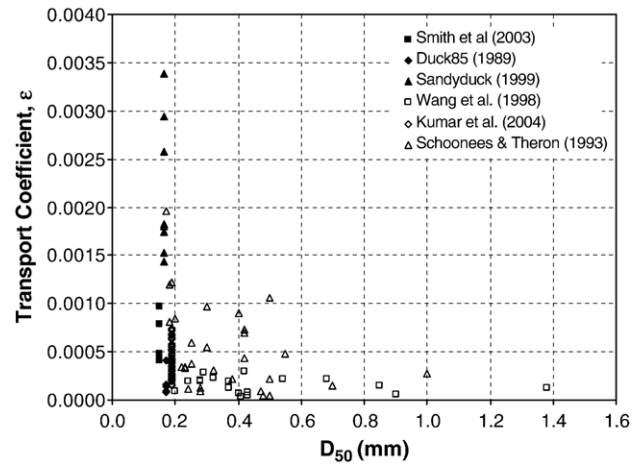

Fig. 3. Relationship between transport coefficient, ε and median grain size, D_{50}.

Hydrodynamic conditions observed during the field experiment are listed in Table 1.

5. Dependence of transport coefficient on governing parameters

Comparison between measured and calculated transport rates with Eq. (7) indicated that the new formula could simulate the data satisfactorily. The dependence on the main governing parameters was correctly described and observed trends reproduced. However, in obtaining the best fit for the formula by selecting an optimal value on the transport coefficient (ε), this value varied markedly between the different experimental cases. Analysis of ε showed that the least-square calculated coefficient values were in the range between 0.00004 and 0.0034 for the studied data sets, indicating that approximately 0.004% to 0.34% of the total wave-energy flux into the surf zone is consumed by the falling grains of suspended sediment. The reasons for the large scatter in the obtained ε-values may be several, including experimental errors, uncertainties in the longshore current computations, unsatisfactory representation of the input conditions, and failure to include all main governing parameters in the formula. With regard to the latter reason, the possible dependence of ε on various physical parameters was investigated and quantified by combining dimensional analysis with empirically based analysis of the data material.

Measured hydrodynamic and sedimentologic properties from each experimental case in the calibration data set were used to investigate the dependence of the transport coefficient (ε) on the main governing parameters, encompassing both dimensional (e.g., wave height, wave period, sediment grain size, settling velocity) and non-dimensional parameters (e.g., ratio of breaking wave height to grain size). Figs. 1 and 2 illustrate the transport coefficient versus significant wave height at breaking ($H_{s,b}$) and peak wave period (T_p), respectively. The figures show that the transport coefficient displays some dependence on the breaking wave height and but less on the wave period. Figs. 3 and 4 depict the transport coefficient versus grain size and grain-settling velocity, respectively. Again, no marked relationship was found between transport coefficient and grain size or grain settling velocity, although there is a

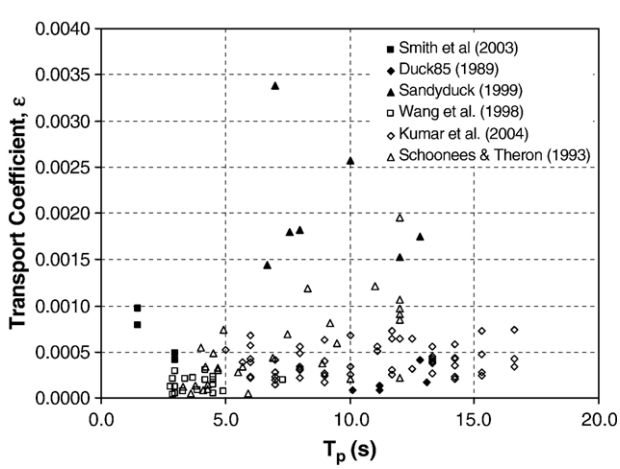

Fig. 2. Relationship between transport coefficient, ε and peak wave period, T_p.

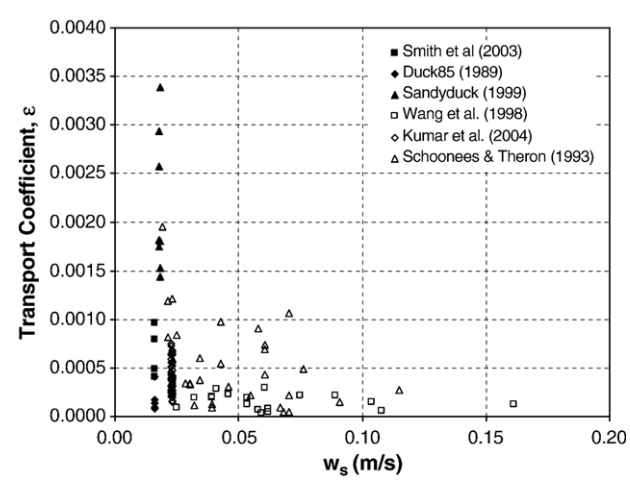

Fig. 4. Relationship between transport coefficient, ε and particle settling velocity, w_s.

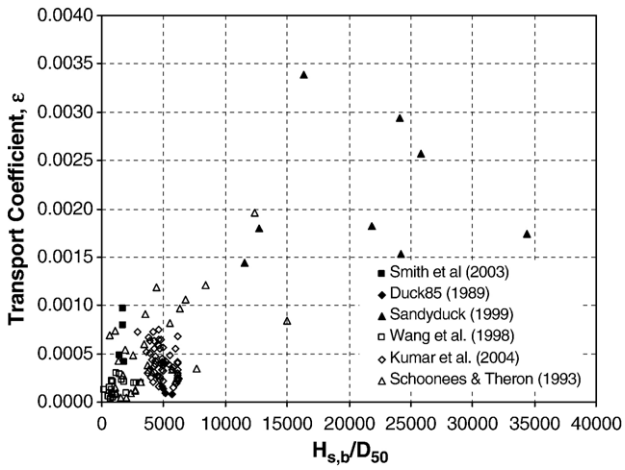

Fig. 5. Relationship between transport coefficient, ε and ratio of breaking wave height to median grain size, $H_{s,b}/D_{50}$.

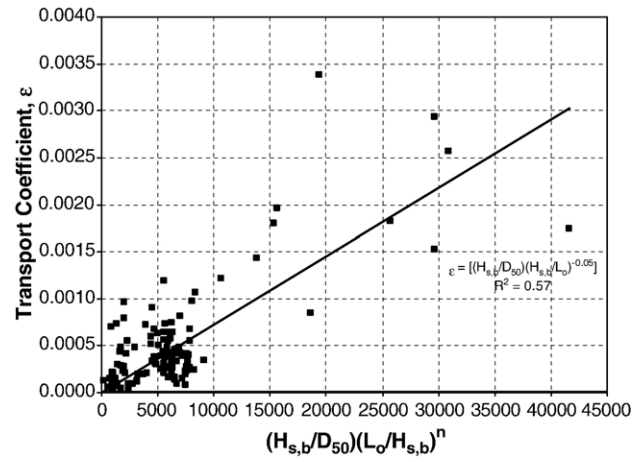

Fig. 7. Relationship between transport coefficient, ε and $(H_{s,b}/D_{50})(L_o/H_{s,b})^n$.

tendency that ε decreases with increasing values on D_{50} on w_s. Although, the scatter is still significant, if the significant wave height at breaking is normalized by the grain size, a linear trend between ε and $H_{s,b}/D_{50}$ is distinguished as illustrated in Fig. 5. In order to proceed with the analysis, a more systematic dimensional analysis was performed to find the non-dimensional quantities that would best describe ε.

The transport coefficient, which expresses the efficiency of the waves in keeping sand grains in suspension, is taken to be a function of the following variables:

$$\varepsilon = f(H_{s,b}, L_o, T_p, h_b, D_{50}, w_s, g, \rho). \tag{20}$$

Dimensional analysis using ρ, g, and $H_{s,b}$ as the primary variables yields,

$$\varepsilon = \phi_1\left(\frac{h_b}{H_{s,b}}, \frac{w_s T_p}{H_{s,b}}, \frac{D_{50}}{H_{s,b}}, \frac{gT_p^2}{H_{s,b}}, \frac{L_o}{H_{s,b}}\right) \tag{21}$$

where ϕ_1 is a function. Since both $H_{s,b}/gT_p^2$ and $H_{s,b}/L_o$ defines the wave steepness, only the former parameter will be considered here. In addition, $H_{s,b}/h_b$ characterizes wave breaking and since by definition only transport in the surf zone is described by the formula, this parameter is not included. Eq. (21) may now be simplified to,

$$\varepsilon = \phi_2\left(\frac{H_{s,b}}{w_s T_p}, \frac{H_{s,b}}{D_{50}}, \frac{H_{s,b}}{L_o}\right) \tag{22}$$

in which $H_{s,b}/w_s T_p$ is known as the Dean number (Dean, 1973). The Dean number and $H_{s,b}/D_{50}$ both express the relative effect of the sediment properties, where the former often is taken to characterize suspended load and the latter bed load. A reasonable fit may be obtained between ε and the Dean number only using the calibration data set. The best fit employing a straight line is given by,

$$\varepsilon = \left(9.0 + 4.0\frac{H_{s,b}}{w_s T_p}\right).10^{-5} \tag{23}$$

with the coefficient of determination $r^2 = 0.63$. Two distinct data clusters are observed in Fig. 6, one with smaller transport rates belonging to moderate wave conditions and one with higher rates from the storm data set collected during the SandyDuck field campaign (Miller, 1999).

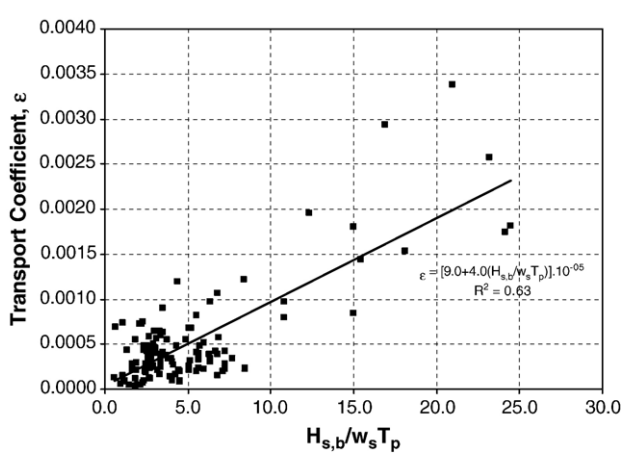

Fig. 6. Relationship between transport coefficient, ε and Dean number $H_{s,b}/w_s T_p$.

Table 2
Summary of predictive capability for all formulas investigated

Formula	Scatter S_{rms}	Trend	Clustering	Data with discrepancy ratio between 1/2 and 2 (%)	Data with discrepancy ratio between 1/4 and 4 (%)
New formula (Eq. (7))	0.13	5.0	5.0	38.0	12.0
CERC (USACE, 1984)	0.70	2.0	2.0	82.0	60.0
Kamphuis (1991)	0.37	4.0	4.0	58.0	25.0
Inman–Bagnold (1963)	0.56	3.0	3.0	78.0	50.0

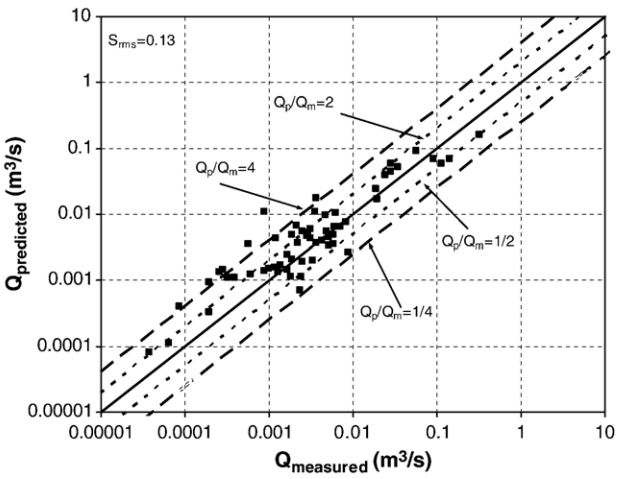

Fig. 8. Measured transport rates versus predicted by the new formula (Eq. (7)) using the verification data set.

Eliminating the Dean number, that is, working with the second and third non-dimensional numbers in Eq. (22), and using successive approximation (Kamphuis, 1991), it can be shown that

$$\varepsilon = \phi_3 \left\{ \left[\frac{H_{s,b}}{D_{50}} \left(\frac{L_o}{H_{s,b}} \right)^n \right]^p \right\} \tag{24}$$

where the exponents were determined to $\Phi_3 = 1$, $p = 1$ and $n = -0.05$ with a coefficient of determination of $r^2 = 0.57$. Fig. 7 shows the relationship between the transport coefficient and the non-dimensional quantity in Eq. (24). Influences of the wave steepness are limited, which can be seen from the low value obtained on n. The coefficient of determination is higher when the Dean number is used compared to $(H_{s,b}/D_{50})(L_o/H_{s,b})^n$. Also, since ε is assumed to represent suspended sediment processes, the Dean number is a better quantity to employ than $H_{s,b}/D_{50}$. Thus, Eq. (23) is recommended for predicting ε and this equation was used in the following comparison with data.

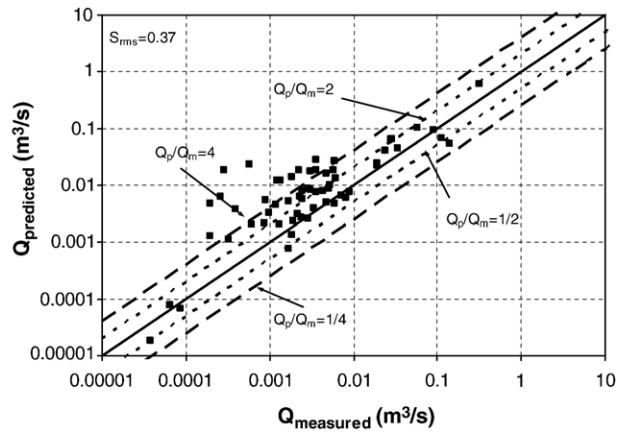

Fig. 10. Measured transport rates versus predicted by the Kamphuis (1991) formula using the verification data set.

6. Comparison between transport predictions and measurements

Comparison with a large quantity of data, covering a wide range of wave, current, sediment, and topographic conditions, was necessary for validating the new LST formula. Thus, the predictive capability of the new formula, with the transport coefficient determined by Eq. (23), was investigated by employing the verification data set compiled in this study. Comparisons were also made with the CERC equation (USACE, 1984) and the formulas proposed by Kamphuis (1991) and Inman and Bagnold (1963).

Quantitative and qualitative comparisons were made between measurements and predictions regarding the scatter, trend, and clustering of the calculated points around the line of

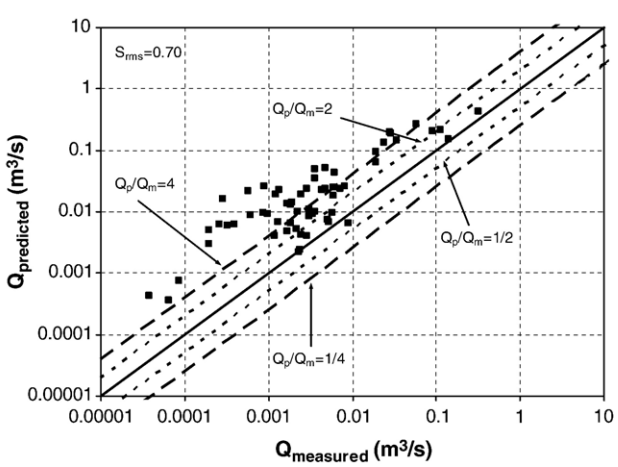

Fig. 9. Measured transport rates versus predicted by the CERC (USACE, 1984) formula using the verification data set.

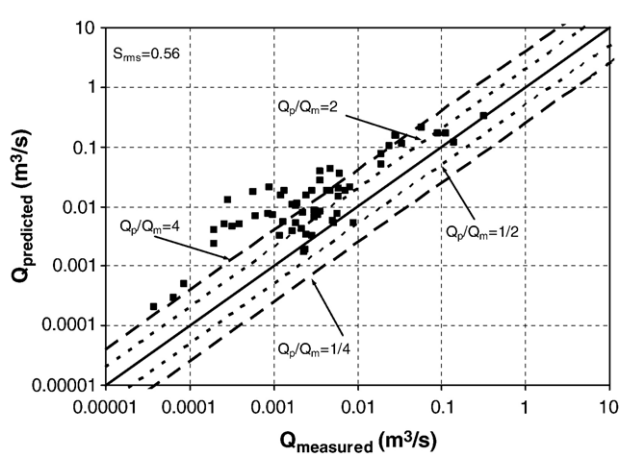

Fig 11. Measured transport rates versus predicted by the Inman-Bagnold (1963) formula using the verification data set.

perfect agreement. As a measure of scatter, the root-mean-square error (S_{rms}) was calculated according to

$$S_{rms} = \sqrt{\frac{\sum_{i=1}^{N} (\log Q_p - \log Q_m)^2}{N-2}} \tag{25}$$

where N is the number of the data points. The computed S_{rms} values for all formulas are listed in Table 2, where a smaller S_{rms} value implies a smaller scatter. From the table it can be seen that present formula exhibits the smallest scatter followed by, in order, the Kamphuis, Bagnold–Inman, and CERC formula.

Based on visual observation (see Figs. 8–11) the formulas were subjectively ranked from 1 (weak) to 5 (strong) concerning trends and clustering. In addition, a mean discrepancy ratio was assigned to the formulas given by the percentage of the measurement points within an interval of 0.5 to 2 of the predictions by the formulas (this value is subtracted from 100% to yield a small number for good agreement).

Fig. 8 shows the predicted versus measured transport rates by the present formulation (Eq. (7)). Most of the computed values are within a factor of 0.5 to 2 of measured values (discrepancy ratio of 38%). The CERC (USACE, 1984) equation has a tendency to overpredict the measured transport rates, and it produced the largest scatter and discrepancy ratio of 82% (Fig. 9). The Kamphuis (1991) formula produced somewhat better predictions than the other two formulas tested having a discrepancy ratio of 58%. Similar to the CERC equation, the Kamphuis formula overpredicted low transport rates (Fig. 10). The Inman-Bagnold (1963) formula had a discrepancy ratio of 78% (Fig. 11). The last column in Table 2 also shows the discrepancy ratio within an interval of 0.25 to 4 of the predictions by the all formulas. Again, the new formula exhibits the smallest discrepancy ratio compared to the other three formulas.

The analytical formula developed here has some clear advantages compared to the CERC equation and the other formulas. It contains a physically based derivation of the grain-size dependence and indirectly through the mean longshore current velocity it includes effects of beach profile shape (e.g., slope). In addition, the new formula can be used to estimate longshore transport rate not only due to breaking waves, but also from currents generated by other forcing mechanisms such as tide and/or wind.

7. Conclusions

A new formula for the total longshore sediment transport (LST) rate was developed based on a simple, yet physically based description of sediment stirring and movement. Suspended load was taken to dominate in the surf zone and steady-state conditions to prevail. It was assumed that the total work needed to keep the grains in suspension is proportional to the incoming wave-energy flux. The product between the local longshore current and the sediment concentration integrated through the vertical and across the surf zone yielded the total longshore transport rate. In order to arrive at a simple formula an average, representative longshore current was assumed. The formula showed that the total transport rate is proportional to the longshore current speed and the incoming wave-energy flux, and that the rate is inversely proportional to the sediment fall speed. Thus, compared to most previous formulas for the total LST rate, the formula proposed in this study exhibit a dependence on the grain size. In addition, transport generated by currents of other origin than from breaking waves, such as tide- and wind-generated currents, may be predicted.

Six data sets from the laboratory and field were compiled as a basis for testing and evaluating the new formula. These data sets were used because of their detail and accuracy, although it should be stressed that sediment transport measurements involve substantial uncertainties. The transport rates in the data sets were measured through either sediment traps or using OBS together with current measurements. Measurements with tracers were discarded because of difficulties to quantify the transport in a reliable manner. In addition, transport data from impoundment studies were not included since they typically yield average values over long periods during which the forcing conditions vary substantially. Comparisons between the new formula and the data sets displayed good agreement. However, least-square fitting of the formula to the data, using the transport rate coefficient as the main parameter to fit, showed that this coefficient varied markedly between the data sets. Thus, some dependence of the transport rate on the governing factors was not captured by the formula, leading to this variation in the optimum coefficient value.

A predictive equation for the transport coefficient was developed by employing dimensional analysis to determine the most important non-dimensional parameters governing the behavior of this coefficient. The Dean number (or dimensionless fall speed) was identified as the leading parameter, and based on the available data on the optimum transport coefficient values a predictive equation was proposed in terms of the Dean number. The empirical parameters in this equation were determined through fitting against 2/3 of the compiled data, whereas 1/3 of the data were employed for verification of the equation. Introducing the empirical equation for the transport coefficient, the new formula yields predictions that lie within a factor of 0.5 to 2 of the measured values for 62% of the data points, which is higher than other commonly employed formulas for the LST rate such as the CERC equation and the formulas developed by Inman–Bagnold and Kamphuis. Employing a simple equation for the mean longshore current velocity in the surf zone generated by breaking waves, the proposed formula reduces to the CERC equation, if a certain relationship between the CERC transport coefficient (K) and the transport coefficient in the new formula holds. In summary, the new formula for calculating the LST rate, where the sediment is mobilized primarily by breaking waves, should be well suited for practical applications in coastal waters, including computing transport rates in numerical models of shoreline change.

Acknowledgments

This work was in part (M.L and H.H) conducted under the Inlet Modeling System Work Unit of the Coastal Inlets Research Program, U.S. Army Corps of Engineers. Dr. Nicholas C. Kraus and Mr. H. Carl Miller were instrumental for compiling and interpreting the Duck85 and SandyDuck field data, respectively. The authors are grateful to Dr. Sanil Kumar of National Institute of Oceanography, India, Dr. Ping Wang, University of South Florida, and Dr. Koos Schoonees, Council for Scientific and Industrial Research, South Africa for providing access to their respective data sets. The authors gratefully acknowledge the help of graduate student Ms. Mushaliza Mustar for compiling the LST database and performing some of the initial analysis. Professor Leo van Rijn provided valuable review comments that significantly improved the study.

References

Ciavola, O., Taborda, R., Ferreira, O., Dias, J.A., 1997. Field measurements of longshore sand transport and control processes on a steep meso-tidal beach in Portugal. Journal of Coastal Research 13 (4), 1119–1129.

Dean, R.G., 1973. Heuristic models of sand transport in the surf zone. Proc. Conf. Eng. Dynamics in the Surf Zone, Sydney, pp. 208–214.

Inman, D.L., Bagnold, R.A., 1963. In: Hill, M.N. (Ed.), "Littoral Processes", in the Sea, vol. 3. Interscience, New York, pp. 529–533.

Kamphuis, J.W., 1991. Alongshore sediment transport rate. Journal of Waterway, Port, Coastal, and Ocean Engineering 117 (6), 624–641.

Kamphuis, J.W., 2002. Alongshore transport of sand. Proceedings of the 28th International Conference on Coastal Engineering. ASCE, pp. 2330–2345.

Katayama, H., Goda, Y., 2000. A sediment pickup rate formula based on energy dissipation rate by random breaking waves. Proceedings of the 27th International Conference on Coastal Engineering. ASCE, pp. 2859–2872.

Komar, P.D., 1998. Beach Processes and Sedimentation. Prentice Hall Inc. 545 pp.

Komar, P.D., Inman, D.L., 1970. Longshore sand transport on beaches. Journal of Geophysical Research 75 (30), 5914–5927.

Kraus, N.C., Gingerinch, K.J., Rosati, J.P., 1989. Duck85 surf zone sand transport experiment. U.S. Army Engineer Waterways Experiment Station, Tech. Report CERC-89-5.

Kriebel, D.L., Kraus, N.C., Larson, M., 1991. Engineering methods for predicting beach profile response. Proceedings of Coastal Sediments '91. ASCE, pp. 557–571.

Kumar, V.S., Anand, N.M., Chandaramohan, P., Naik, G.N., 2004. Longshore sediment transport rate; measurements and estimation Central West Coast of India. Coastal Engineering 48, 95–104.

Larson, M., Bayram, A., 2005. Calculating cross-shore distribution of longshore sediment transport. In: Bruun, P. (Ed.), Port and Coastal Engineering, Developments in Science and Technology. Journal of Coastal Research Special Issue, vol. 46, pp. 203–235.

Larson, M., Hanson, H., 1996. Schematized Numerical Model of Three-dimensional Beach Change. 10th Congress of the IAHR Asia and Pacific Division, Langkawi Island, Malaysia, vol. 2, pp. 325–332.

Larson, M., Kraus, N., 1991. Numerical model of longshore current for bar and trough beaches. Journal of Waterway, Port, Coastal and Ocean Engineering 117 (4), 326–347.

Longuet-Higgins, M.S., 1970. Longshore current generated by obliquely incident sea waves. 1. Journal of Geophysical Research 75 (33), 6778–6789.

Masselink, G., Pattiarachi, C., 1998. The effect of sea breeze on beach morphology, surf zone hydrodynamics and sediment re-suspension. Marine Geology 146, 115–135.

Miller, H.C., 1998. Comparison of storm longshore transport rates to predictions. Proceedings of the 26th International Conference on Coastal Engineering. ASCE, pp. 2954–2967.

Miller, H.C., 1999. Field measurements of longshore sediment transport during storm. Coastal Engineering 36, 301–321.

Schoonees, J.S., Theron, A.K., 1993. Review of the field-data base for longshore sediment transport. Coastal Engineering 19, 1–25.

Schoonees, J.S., Theron, A.K., 1996. Improvement of the Most Accurate Longshore Transport Formula. 25th International Conference on Coastal Engineering, vol. 3. ASCE, Orlando, FL, pp. 3652–3665.

Smith, E.R., Wang, P., Zhang, Jun, 2003. Evaluation of the CERC formula using large-scale model data. U.S. Army Engineer Research and Development Center, Coastal and Hydraulics Laboratory, Vicksburg.

USACE, 1984. Shore Protection Manual. Department of the Army, U.S. Corps of Engineers, Washington, DC 20314.

Van Rijn, L.C., 1993. Principles of Sediment Transport in Rivers, Estuaries, and Coastal Seas. Aqua Publications, Amsterdam.

Wang, P., Kraus, N.C., Davis Jr., R.A., 1998. Total longshore sediment transport rate in the surf zone: field measurements and empirical predictions. Journal of Coastal Research 14 (1), 269–282.

Wang, P., Ebersole, B.A., Smith, E.R., 2002. Longshore sand transport — initial results from large-scale sediment transport facility. U.S. Army Corps of Engineers, ERDC/CHL CHETN-II-46. 10 pp.